

SIMCLUST – A PROGRAM TO SIMULATE STAR CLUSTERS

V. Deveikis¹, D. Narbutis^{1,2}, R. Stonkutė², A. Bridžius² and V. Vansevicius^{1,2}

¹ *Vilnius University Observatory, Čiurlionio 29, Vilnius LT-03100, Lithuania*
viktoras.deveikis@ff.vu.lt

² *Institute of Physics, Savanorių 231, Vilnius LT-02300, Lithuania*

Received 2008 November 18; accepted 2008 December 30

Abstract. We present a program tool, SIMCLUST, designed for Monte-Carlo modeling of star clusters. It populates the available stellar isochrones with stars according to the initial mass function and distributes stars randomly following the analytical surface number density profile. The tool is aimed at simulating realistic images of extragalactic star clusters and can be used to: (i) optimize object detection algorithms, (ii) perform artificial cluster tests for the analysis of star cluster surveys, and (iii) assess the stochastic effects introduced into photometric and structural parameters of clusters due to random distribution of luminous stars and non-uniform interstellar extinction. By applying SIMCLUST, we have demonstrated a significant influence of stochastic effects on the determined photometric and structural parameters of low-mass star clusters in the M31 galaxy disk. The source code and examples are available at the SIMCLUST website: <http://www.astro.ff.vu.lt/software/simclust/>.

Key words: galaxies: star clusters – galaxies: individual (M31) – methods: numerical – techniques: photometric

1. INTRODUCTION

Recent studies of star clusters have extended our understanding of these gravitationally bound systems, which have also been successfully used to investigate evolution of their host galaxies; see a review by Kroupa (2008) and references therein. The recent observational data (see review by Renzini 2008) suggest the presence of multiple stellar populations in star clusters. Theoretical modeling (e.g., Lamers et al. 2006; Kruijssen & Lamers 2008) indicates that the stellar mass function evolves from the initial mass function (IMF) due to dynamical effects as the cluster ages. However, the assumption that a star cluster consists of a simple stellar population (SSP) is still an attractive simplification in extragalactic studies.

Although due to the improved quality of observations the detection of extensive low-mass extragalactic star cluster samples is now possible, the straightforward application of SSP models to derive their evolutionary parameters is valid only for high-mass clusters (Cerviño & Luridiana 2004), even neglecting effects of dynamical evolution and loss of stars. The morphology of young low-mass star clusters also depends on the stochastic distribution of luminous stars and non-uniform extinction, therefore, their structural, as well as photometric parameters are biased.

These stochastic uncertainties are also very important for the study of selection effects in extragalactic surveys of unresolved and semi-resolved star clusters, which should be quantified in terms of age, mass, extinction and size.

Therefore, we have developed a program tool, SIMCLUST, by adopting Monte-Carlo modeling, which was previously used to study cluster color distributions (e.g., Girardi & Bica 1993; Bruzual 2002), but extending this approach to simulate *realistic* images. Thus, proper investigation of stochastic effects and observational errors on structural parameters and aperture CCD photometry, as well as the effects of non-uniform extinction in a star cluster, become now possible. The program code is available under the GNU license¹ and may be modified to incorporate different isochrones and stellar surface number density distribution profiles. The source code and examples are available at the SIMCLUST website².

SIMCLUST was applied to investigate stochastic effects and the validity of the SSP model fitting for compact star cluster sample in the disk of the M31 galaxy (Narbutis et al. 2008). In this study we have simulated numerous images of artificial clusters of typical age, mass and size, characteristic of the M31 clusters (Vansevičius et al. 2009). Significant influence of stochastic effects was found for low-mass ($\lesssim 3000 M_{\odot}$) star clusters younger than ~ 100 Myr.

This program tool shares a similar approach to the star cluster simulation problem investigated by Popescu & Hanson (2008). SIMCLUST uses different stellar isochrone sets, initial mass function sampling technique and modeling of interstellar extinction, thus the user is provided with an independent tool to perform Monte-Carlo simulations of extragalactic star clusters and to check the robustness of cluster models.

We present the star cluster simulation method in §2, describe the SIMCLUST program in §3 and investigate stochastic effects for cluster sample in the M31 galaxy in §4. We also discuss the implications of Monte-Carlo modeling in extragalactic star cluster studies on both the estimation of star cluster sample completeness and determination of object parameters in the stochastic model framework.

2. STAR CLUSTER SIMULATION

SIMCLUST program populates a stellar isochrone of a given age and metallicity with stars. Randomly generated masses of stars are weighted on the IMF and the process is repeated until a given mass of model star cluster, M , is reached. Stellar magnitudes are computed assuming a distance to the artificial “extragalactic” cluster, and stars are scattered in the image plane by the analytical surface number density profile. The effect of non-uniform extinction can be applied for individual stars. Finally, *realistic* multi-band images of model cluster are rendered. We describe the details of each step below.

2.1. Isochrones and extinction – stellar magnitudes

For stellar magnitudes in different photometric passbands as a function of *initial*³ stellar mass in solar-mass unit, m , age, t , and metallicity, $[M/H]$, we use a new set of Padova⁴ isochrones by Marigo et al. (2008). These isochrones are

¹ GNU General Public License.

² Download SIMCLUST from <http://www.astro.ff.vu.lt/software/simclust/>.

³ Initial and actual (smaller due to mass loss) stellar masses are provided in isochrone tables.

⁴ Padova isochrones: <http://stev.oapd.inaf.it/cgi-bin/cmd>.

combined of models: (i) up to early-AGB from Girardi et al. (2000), (ii) detailed TP-AGB for $m \leq 7 M_{\odot}$ from Marigo & Girardi (2007) and (iii) for $m > 7 M_{\odot}$ from Bertelli et al. (1994), and take into account many critical aspects of AGB evolution, important for star cluster simulations. In this study we have used the Marigo et al. (2008) isochrones in the Johnson-Cousins *UBVR_IJHK* photometric system (Maíz Apellániz 2006; Bessell 1990).

The isochrone consists of points for a discrete stellar mass with tabulated corresponding magnitudes for each passband. For every randomly generated star (see § 2.2), we calculate its magnitude in each passband by linear interpolation between the closest mass points on the isochrone. The accuracy of the magnitude is directly related to the mass sampling on the isochrone, and the linear interpolation should have negligible effect on the accuracy of the integrated cluster magnitude.

The interstellar extinction is applied for individual stars assuming the standard extinction law (Cardelli et al. 1989), calculated as a function of the given color excess, E_{B-V} . To investigate the effects of non-uniform (differential) extinction in young clusters (Yadav & Sagar 2001), we assume for simplicity that reddening of individual stars in the cluster is described by a Gaussian distribution over mean E_{B-V} and a standard deviation $\sigma_{E_{B-V}}$. This distribution is generated using `gsl_ran_gaussian` function from the GNU Scientific Library⁵. Setting the $\sigma_{E_{B-V}} = 0$, all stars are reddened by the same amount. In case of $\sigma_{E_{B-V}} > 0$, the lower limit of reddening, corresponding to the foreground extinction, is applied.

2.2. IMF – stellar mass distribution

The stellar initial mass function defines a number of stars, dN , within a stellar mass range, dm . In this work we use the universal IMF (Kroupa 2001), defined as the multi-power law, which has the general form of

$$\xi(m) = dN/dm = C_{\text{IMF}} \cdot b_i \cdot m^{\alpha_i}, \quad (1)$$

where α_i is the IMF slope for the mass interval $[m_{i-1}, m_i]$, C_{IMF} and b_i are the normalization and function continuation constants, respectively.

We follow the practical numerical formulation of the IMF by Pflamm-Altenburg & Kroupa (2006), and implement their shared library “Libimf”⁶ in our code; namely the function `imf_init_multi_power`, which allows us to define an arbitrary number i of mass intervals $[m_{i-1}, m_i]$, and corresponding power law slopes α_i .

Because of the lowest stellar mass limit $m_{\text{min}} = 0.15 M_{\odot}$ for the isochrones used, the IMF slope (Eq. 2, Kroupa 2001) transforms into a simple equation:

$$\begin{cases} \alpha_0 = -1.3, & m/M_{\odot} < 0.50; \\ \alpha_1 = -2.3, & m/M_{\odot} \geq 0.50. \end{cases} \quad (2)$$

Before a random number generator can be applied to sample the IMF, it has to be normalized, i.e., the constant C_{IMF} has to be defined. We follow the normalization strategy by Weidner & Kroupa (2004), implemented by Pflamm-Altenburg & Kroupa (2006) in the “Libimf” library as a function `imf_norm_wk04`. It requires two additional free parameters: (i) $m_{\text{max}*} = 150 M_{\odot}$ – the maximum physically possible stellar mass, and (ii) m_{max} – the expected maximum stellar mass in a

⁵ GSL version 1.9: <http://www.gnu.org/software/gsl/>.

⁶ Libimf: <http://www.astro.uni-bonn.de/~webaiub/dwld/libimf-05-10-06.tar.gz>.

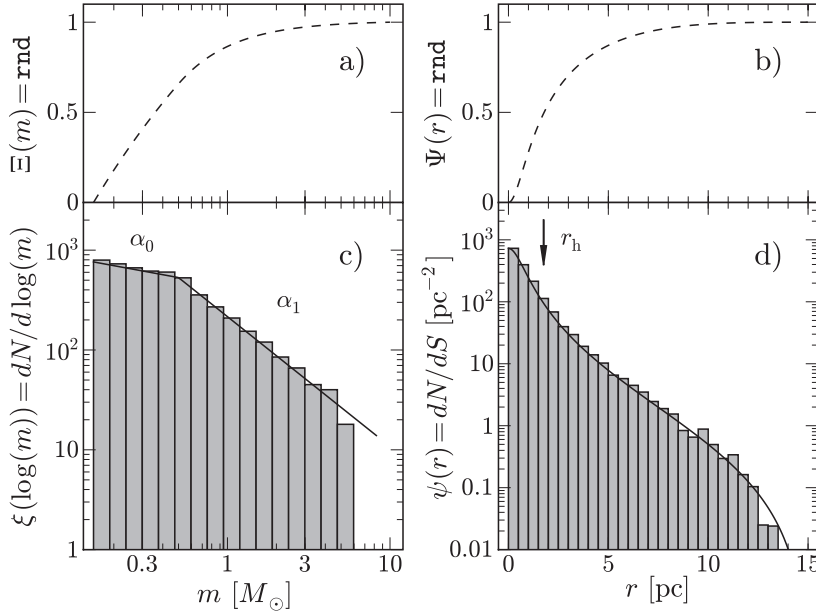


Fig. 1. Properties of a model star cluster with $t = 100$ Myr and “luminous” mass $M_{\text{lum}} = 3000 M_{\odot}$, consisting of $N_{\text{lum}} = 5300$ stars. The cumulative mass distribution function $\Xi(m)$ of the IMF (see Eq. 3) and the cumulative radial distribution function $\Psi(r)$ of the King model (see Eq. 6), displayed in panels (a) and (b), respectively, are used to sample mass, m , and radial distance, r , by means of uniform random numbers, `rnd`. The stellar mass distribution, $\xi(\log(m)) = dN/d \log(m)$, is displayed vs. mass, m , in panel (c), overplotted with slope $\alpha_0 = -1.3$ and $\alpha_1 = -2.3$ lines of IMF (see Eq. 2). The lower and upper mass limits are defined by the isochrone. The surface number density of stars, $\psi(r) = dN/dS$, is plotted vs. radial distance, r , in panel (d), obeying King (1962) model profile of $r_c = 0.75$ pc and $r_t = 15$ pc (see Eq. 5); half-light radius $r_h \sim 1.7$ pc is indicated by an arrow.

given cluster of mass M . A reasonable assumption is to define both C_{IMF} and m_{max} in such a way, that there is *only one* massive star of mass m_{max} in the mass range $[m_{\text{max}}, m_{\text{max}^*}]$. Thus, the expected maximum stellar mass is a function of cluster’s mass, i.e., $m_{\text{max}} = m_{\text{max}}(M)$. The normalization is a required procedure for the present application of the Monte-Carlo method, since now the IMF can be treated as a probability density function in the range between m and $m + dm$.

The IMF sampling technique can be summarized as follows: from Eq. 1 a cumulative mass distribution function, giving a probability that mass $m' \leq m$, is constructed:

$$\Xi(m) = \int_{m_{\text{min}}}^m \xi(m') dm'. \quad (3)$$

This function (Eq. 3) is continuous between 0 and 1 (see Figure 1a). Thus, a uniform random number, `rnd`, obtained from long periodicity `gsl_rng_taus` randomizer function of the GNU Scientific Library, is attributed to $\Xi(m) = \text{rnd}$. The

stellar mass m values are sampled from the IMF via inverse function

$$m = F^{-1}(\Xi(m) = \text{rnd}) , \quad (4)$$

which has an analytical solution. We use the ‘‘Libimf’s’’ `imf_dice_star_cl` function to generate an array of stellar masses according to the supplied IMF.

The mass of the cluster derived by the SSP model fitting and used in population analysis is usually the initial mass at the cluster’s birth. Following this definition, we generate the initial mass function of stars at age $t = 0$ Myr, where individual stellar masses populate the range $[m_{\min}, m_{\max}]$, as defined previously. We denote the sum of initial stellar masses to the mass of the cluster, M . When the isochrone of age $t > 0$ Myr is sampled, only stars, which are present at that age ($m_{\max} = m_{\max}(t) < m_{\max}(t = 0 \text{ Myr})$) contribute to the luminosity of cluster, i.e., ‘‘luminous’’ mass, M_{lum} , is always lower than the ‘‘initial’’ mass, M , of the cluster. Also, the mass-loss of stars due to stellar winds can be accounted for and directed to the output.

An example of the resulting stellar mass distribution, $\xi(\log(m)) = dN/d \log(m)$, displayed vs. mass, m , of $t = 100$ Myr model star cluster of ‘‘luminous’’ mass $M_{\text{lum}} = 3000 M_{\odot}$, consisting of $N_{\text{lum}} = 5300$ stars, is shown in Figure 1c, overplotted with the IMF slope $\alpha_0 = -1.3$ and $\alpha_1 = -2.3$ lines (see Eq. 2).

2.3. Radial surface number density profile – 2-D spatial distribution

Once the mass and multi-band magnitudes of a star are known, its spatial position has to be defined. For simplicity we assume that the ‘‘observed’’ positions of the stars are distributed randomly in the 2-D plane, obeying a circular King (1962) model.

The King model describes the radial surface number density profile, i.e., the number of stars, dN , per unit area, dS and is defined by the central surface number density, ψ_0 , the core radius, r_c , and the tidal radius, r_t :

$$\psi(r) = dN/dS = dN/2\pi r dr = \psi_0 \left[\left(1 + \frac{r^2}{r_c^2}\right)^{-1/2} - \left(1 + \frac{r_t^2}{r_c^2}\right)^{-1/2} \right]^2 , \quad (5)$$

where r is the distance from cluster’s center.

The cumulative radial distribution function of the circular King model giving probability that the distance $r' \leq r$, is defined by formula:

$$\begin{aligned} \Psi(r) &= 2\pi C_{\text{King}} \int_0^r r' \psi(r') dr' = \\ &\pi C_{\text{King}} \cdot r_c^2 \left[\ln(1 + (r/r_c)^2) - 4 \left(\sqrt{(r_c^2 + r^2)/\lambda} - \sqrt{r_c^2/\lambda} \right) + r^2/\lambda \right] , \end{aligned} \quad (6)$$

where $\lambda = r_c^2 + r_t^2$, and C_{King} is the normalization constant, defined as

$$C_{\text{King}} = \left(2\pi \int_0^{r_t} r' \psi(r') dr' \right)^{-1} . \quad (7)$$

The $\Psi(r)$ function (Eq. 6) is continuous between 0 and 1 (see Figure 1b). Thus, a uniform random number, `rnd`, is attributed to $\Psi(r) = \text{rnd}$ to sample the distance r values from the King model via inverse function

$$r = F^{-1}(\Psi(r) = \text{rnd}) , \quad (8)$$

which does not have an analytical expression. Since the function $\Psi(r)$ is monotonously increasing, therefore, for a generated random number, `rnd`, we can solve Eq. 8 via Eq. 6, iteratively by the bisection method until the solution of r converges.

An example of the resulting surface number density of stars, $\psi(r) = dN/dS$, displayed vs. radial distance, r , of the model star cluster, consisting of $N_{\text{lum}} = 5300$ stars, is shown in Figure 1d, overplotted with the King (1962) model profile of $r_c = 0.75$ pc and $r_t = 15$ pc (see Eq. 5); half-light⁷ radius $r_h \sim 1.7$ pc is indicated by an arrow.

Finally, the azimuth angle, φ , is assigned randomly for a star. Stellar positions in parsecs (x, y) are computed in respect to the cluster center:

$$\begin{cases} \varphi = 2\pi \cdot \text{rnd} , \\ x = r \cdot \cos(\varphi) , \\ y = r \cdot \sin(\varphi) . \end{cases} \quad (9)$$

2.4. Realistic images

The distance to the star cluster, D , and the photometric zero-point are used to transform the absolute magnitudes of stars to the instrumental magnitude system in each photometric passband. Stellar positions in the image are computed assuming the provided pixel scale, θ , and the center coordinates of star cluster.

Finally, these data are passed to the external “SkyMaker”⁸ program, which renders *realistic* images for each photometric passband, assuming the provided point-spread function (PSF). Usually the PSF is derived from the real image by using the DAOPHOT program package (Stetson 1987) implemented in the IRAF program system (Tody 1993). Since “SkyMaker” has many image rendering options, they can be used to create realistic image noise properties, or even simulate images for an arbitrary telescope configuration or observational conditions.

3. SIMCLUST – PROGRAM DESCRIPTION

Here we present a short description of SIMCLUST usage, the properties of input files, parameter configuration and output files. The schematic representation of the data flow is shown by means of a block diagram given in Figure 2.

SIMCLUST is written in the Perl and C++ languages and can be compiled under the “UNIX/Linux” systems. Installation script `compile` checks that external program “SkyMaker” and all necessary libraries are available on the computer and builds executables. The configuration file `example`, which contains main parameters of the model star cluster and instructions on how the images should be simulated, is passed to `SimClust` which controls two sub-programs, `CLSCREATOR` and `FITSCREATOR`.

⁷ In this case this is the radius containing the half number of the stars.

⁸ SkyMaker version 3.1.0: <http://terapix.iap.fr/soft/skymaker>.

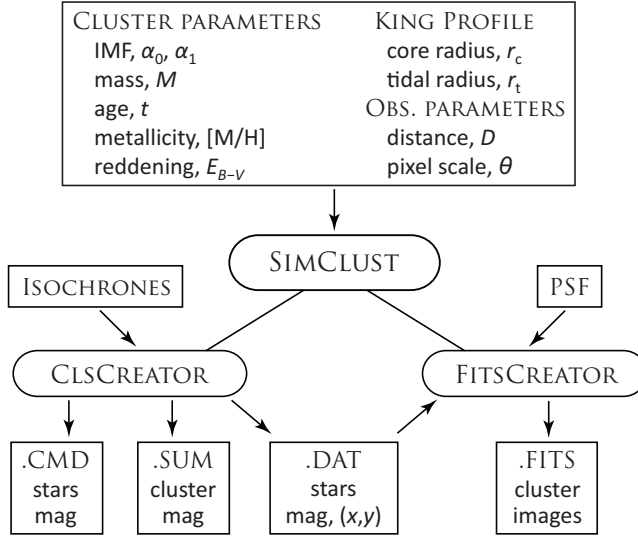


Fig. 2. Schematic representation of SIMCLUST, which consists of two sub-programs – CLSCREATOR and FITSCREATOR. Arrows indicate the parameter and data flow.

The CLSCREATOR, which randomly populates the input stellar isochrones, has to be executed first. There are three possible output options: (i) `.cmd` file, containing magnitudes of individual stars, (ii) `.sum` – integrated magnitudes of star clusters, and (iii) `.dat` – stellar magnitudes and positions. Later the FITSCREATOR can be asked to pass `.dat` files and PSF to the “SkyMaker” to simulate cluster images (`.fits`).

The detailed description of each configuration parameter is documented in the help file and illustrated with examples.

4. STOCHASTIC EFFECTS OF STAR CLUSTERS

The accuracy of cluster age and mass from broad-band photometry, derived by applying traditional SSP models, as well as the accuracy of structural cluster parameters, depend on the clusters age, mass and size, image spatial resolution, data analysis techniques and stochastic effects. To account properly for stochastic effects, we have developed SIMCLUST and applied it to investigate properties of star clusters in the extensively studied South-West field of the M31 galaxy (Kodaira et al. 2004, 2008; Narbutis et al. 2006, 2007b, 2008). Previously, for this cluster sample the influence of individual semi-resolved bright stars on the accuracy of the structural cluster parameters was discussed by Šablevičiūtė et al. (2006, 2007), and the influence on the accuracy of aperture photometry was studied by Narbutis et al. (2007a).

In the following we provide an example of SIMCLUST application to study star clusters in M31. We describe the cluster simulations and the expected photometric and half-light radii uncertainties, derived for typical star clusters of our sample. For the present study we assume the typical parameter values of compact star clusters (Vansevicius et al. 2009): age ~ 100 Myr, mass $\sim 3000 M_{\odot}$ and half-light radius ~ 1.5 pc.

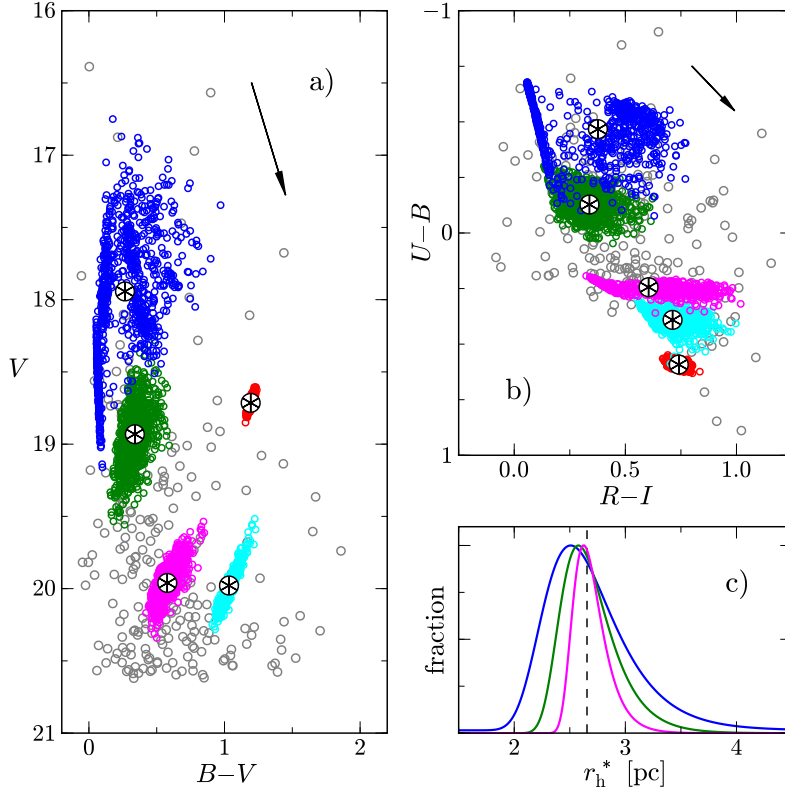


Fig. 3. Modeling of stochastic effects. Panel (a). The diagram V vs. $B-V$ of 238 high probability star cluster candidates in M31 (gray circles) from Vanevičius et al. (2009), overplotted with five cases of model clusters for the ages $t = 20, 100, 500$ Myr, 2.5 and 12.5 Gyr, and “luminous” masses $\log(M_{\text{lum}}/M_{\odot}) = 3.5, 3.5, 3.5, 4.0$ and 5.0 (blue, green, magenta, cyan and red symbols), 1000 models for each case. Asterisks indicate the position of the SSP model, vector indicates interstellar reddening of $E_{B-V} = 0.25$. Panel (b). The diagram $U-B$ vs. $R-I$, symbols are the same as in (a). Panel (c). Distributions of model clusters half-light radii, measured using a curve-of-growth method, for the ages $t = 20, 100$ and 500 Myr; the dashed line indicates the true $r_h^* = 2.6$ pc.

4.1. Star cluster model setup

Since the majority of objects in the M31 sample are young low-mass star clusters, we were motivated to investigate the influence of stochastic distribution of bright stars on both photometric and structural properties. For this purpose, we have chosen parameters adequate to the characteristic values of our sample: (i) five age cases, $t = 20, 100, 500$ Myr, 2.5 and 12.5 Gyr; (ii) “luminous” masses, which correspond to the adopted ages, $\log(M_{\text{lum}}/M_{\odot}) = 3.5, 3.5, 3.5, 4.0$ and 5.0; (iii) metallicity, $[M/H] = -0.4$ dex; (iv) reddening, $E_{B-V} = 0.25$; (v) distribution of stars according to the circular King model of $r_c = 0.75$ pc and $r_t = 15$ pc, i.e., $r_h \approx 1.7$ pc. A thousand model clusters were produced for each age-mass cases.

Model star clusters were placed at the distance of M31, $D = 785$ kpc, derived by McConnachie et al. (2005); thus $1'' = 3.8$ pc. For simplicity, zero photometric background and noise was assumed for image simulation.

4.2. Photometric properties

To examine the photometric properties of model clusters, images equivalent to the Local Group Galaxies Survey data (Massey et al. 2006) with homogenized PSF of FWHM $\approx 1.5''$ were simulated; image scale $\theta = 0.27''$ per pixel. The *UBVRI* photometry was performed with IRAF's `phot` through apertures of $3''$ in diameter – a typical size used for the sample clusters (see Narbutis et al. 2008 for details of photometry).

The resulting diagrams V vs. $B-V$ and $U-B$ vs. $R-I$ are displayed in Figures 3a and 3b, respectively, overplotted on 238 high probability cluster candidates, selected by Vansevičius et al. (2009). The stochastic scatter of model luminosity and color dominates over the typical photometric errors. The indicated SSP model points⁹ (Marigo et al. 2008) of $[M/H] = -0.4$ dex, reddened by $E_{B-V} = 0.25$, show that SSP colors at $t = 20$ Myr and 500 Myr do not represent model cluster colors and are disturbed asymmetrically around the SSP position in two-color diagram due to stochastic existence of bright blue and red supergiants, RGB and AGB stars, prominent at these ages. However, for the remaining three model ages, the centers of color distribution coincide well with the SSP models. The color distribution of sample clusters is covered by the extent of stochastic models with assumed typical reddening of $E_{B-V} = 0.25$. We note, that the scatter of colors of $t = 100$ Myr and $\log(M_{\text{lum}}/M_{\odot}) = 3.5$ models resemble that of real objects located around $[0.4, -0.2]$ in Figure 3b.

4.3. Structural properties

To examine the structural properties of model clusters, images equivalent to the Suprime-Cam V -band data of FWHM_{PSF} $\approx 0.7''$ were simulated; the image scale $\theta = 0.20''$ per pixel (see Narbutis et al. 2008 for Suprime-Cam survey data details).

IRAF's `phot` was applied to obtain the profile of the enclosed flux of a cluster model using the curve-of-growth method, yielding the half-light radius, r_h^* . Note, however, that observational effects (PSF) were not taken into account.

The derived half-light radii r_h^* data histograms of 10^3 models for ages $t = 20, 100$ and 500 Myr were constructed. After smoothing, they are displayed in Figure 3c. The scatter around the true $r_h^* \approx 2.6$ pc value is due to a stochastic distribution of bright stars in model star clusters. The stochastic effect is most significant for the $t = 20$ Myr models, and decreases to older and more massive clusters. The values of r_h^* are smaller for clusters, which have bright stars residing in the cluster centers, dominating the overall luminosity. Contrary, when bright stars are located far from the center, the derived r_h^* values are increased. The standard deviation of r_h^* distribution of the youngest model clusters ($t = 20$ Myr) is ~ 0.5 pc and decreases to ~ 0.1 pc for the oldest ones ($t = 500$ Myr).

5. DISCUSSION AND CONCLUSIONS

Simulations of star cluster images are becoming important to evaluate the performance of analysis techniques of observational data, as have been shown by, e.g., Ascenso et al. (2008) for the case of mass segregation in star clusters. Popescu & Hanson (2008) emphasize the importance of realistic star cluster simulation with

⁹ Padova SSP models: <http://stev.oapd.inaf.it/cgi-bin/cmd>.

incorporation of interstellar extinction to answer the question about the lack or existence of massive star clusters in galaxies. The current knowledge about the most massive clusters can be limited due to unknown selection effects.

There is no technique available (Cerviño & Luridiana 2006) to properly account for stochastic effects when photometric data are interpreted in the framework of SSP models, except of star cluster simulation and assessment of the reliability of the SSP model performance in certain age and mass domains. It might turn-out that the interpretation of properties of the cluster population, especially in the young low-mass domain, will change dramatically once the stochastic effects are taken into account. On the other hand, the fundamental limitation on the amount of information, which can be extracted from integrated photometry alone, will be established and other techniques shall be developed.

It should be emphasized here, that even for the high-mass star clusters, where stochastic uncertainties are comparable to the observation photometric errors, parameter degeneracies in broad-band photometry are unavoidable; see Bridžius et al. (2008) for the performance analysis of the *UBVRIJHK* photometric system.

The tests performed in this study show that the stochastic effects are significant for low-mass young clusters. The age degeneracy due to stochastic color scatter is observed in all model cases. The reddening vector in Figure 3 implies that stochastic color shift could also mimic reddening. Therefore, when SSP model fitting is applied, the derived cluster mass becomes more uncertain, not only due to the miss-match of age and extinction, but also due to the intrinsic scatter of luminosity. Visual inspection of the model cluster color images shows a close resemblance to the real compact cluster candidates in respect to their semi-resolved appearance and stochastic emergence of bright blue or red stars.

The morphology of low-mass star clusters is strongly dependent on the stochastic distribution of luminous stars and the spatial resolution of the image. A usual “by-eye” selection technique leads to systematic biases in the magnitude limited samples, thus automatic detection should be used instead. To properly estimate the completeness of cluster sample, the artificial star cluster tests should be performed using *realistic* simulations of cluster images on individual star basis, instead of just assuming the smooth surface brightness distribution profiles.

The stochastic SSP model framework, which could replace the traditional SSP model fitting to quantify ages, masses and extinctions of star clusters from their integrated broad-band photometry, is still to be developed. The *SIMCLUST* program tool may serve as a basis for this method, as well as for extensive extragalactic star cluster studies.

ACKNOWLEDGMENTS. We thank A. Kučinskas for critical comments and numerous suggestions, which helped to improve the paper. This work was financially supported in part by a Grant of the Lithuanian State Science and Studies Foundation.

REFERENCES

- Ascenso J., Alves J., Lago M. T. V. T. 2008, arXiv:0811.3213
Bertelli G., Bressan A., Chiosi C., Fagotto F., Nasi E. 1994, *A&AS*, 106, 275
Bessell M. S. 1990, *PASP*, 102, 1181

- Bridžius A., Narbutis D., Stonkutė R., Deveikis V., Vansevicius V. 2008, *Baltic Astronomy*, 17, 337
- Bruzual A. G. 2002, in *Extragalactic Star Clusters*, IAU Symp. 207, Eds. D. Geisler et al., ASP, p. 616
- Cardelli J. A., Clayton G. C., Mathis J. S. 1989, *ApJ*, 345, 245
- Cerviño M., Luridiana V. 2004, *A&A*, 413, 145
- Cerviño M., Luridiana V. 2006, *A&A*, 451, 475
- Girardi L., Bica E. 1993, *A&A*, 274, 279
- Girardi L., Bressan A., Bertelli G., Chiosi C. 2000, *A&AS*, 141, 371
- King I. 1962, *AJ*, 67, 471
- Kodaira K., Vansevicius V., Bridžius A., Komiyama Y., Miyazaki S., Stonkutė R., Šablevičiūtė I., Narbutis D. 2004, *PASJ*, 56, 1025
- Kodaira K., Vansevicius V., Stonkutė R., Narbutis D., Bridžius A. 2008, in *Panoramic Views of Galaxy Formation and Evolution*, ASP Conf. Ser., 399, 431
- Kroupa P. 2001, *MNRAS*, 322, 231
- Kroupa P. 2008, arXiv:0810.4143
- Kruijssen J. M. D., Lamers H. J. G. L. M. 2008, *A&A*, 490, 151
- Lamers H. J. G. L. M., Anders P., de Grijs R. 2006, *A&A*, 452, 131
- McConnachie A. W., Irwin M. J., Ferguson A. M. N., Ibata R. A., Lewis G. F., Tanvir N. 2005, *MNRAS*, 356, 979
- Maíz Apellániz J. 2006, *AJ*, 131, 1184
- Marigo P., Girardi L. 2007, *A&A*, 469, 239
- Marigo P., Girardi L., Bressan A., Groenewegen M. A. T., Silva L., Granato G. L. 2008, *A&A*, 482, 883
- Massey P., Olsen K. A. G., Hodge P. W., Strong S. B., Jacoby G. H., Schlingman W., Smith R. C. 2006, *AJ*, 131, 2478
- Narbutis D., Vansevicius V., Kodaira K., Šablevičiūtė I., Stonkutė R., Bridžius A. 2006, *Baltic Astronomy*, 15, 461
- Narbutis D., Vansevicius V., Kodaira K., Bridžius A., Stonkutė R. 2007a, *Baltic Astronomy*, 16, 409
- Narbutis D., Bridžius A., Stonkutė R., Vansevicius V. 2007b, *Baltic Astronomy*, 16, 421
- Narbutis D., Vansevicius V., Kodaira K., Bridžius A., Stonkutė R. 2008, *ApJS*, 177, 174
- Pflamm-Altenburg J., Kroupa P. 2006, *MNRAS*, 373, 295
- Popescu B., Hanson M. M. 2008, arXiv:0811.4210
- Renzini A. 2008, *MNRAS*, 391, 354
- Stetson P. B. 1987, *PASP*, 99, 191
- Šablevičiūtė I., Vansevicius V., Kodaira K., Narbutis D., Stonkutė R., Bridžius A. 2006, *Baltic Astronomy*, 15, 547
- Šablevičiūtė I., Vansevicius V., Kodaira K., Narbutis D., Stonkutė R., Bridžius A. 2007, *Baltic Astronomy*, 16, 397
- Tody D. 1993, *Astronomical Data Analysis Software and Systems II*, 52, 173
- Vansevicius V., Kodaira K., Narbutis D., Stonkutė R., Bridžius A., Deveikis V., Semionov D. 2009, *ApJ*, submitted
- Weidner C., Kroupa P. 2004, *MNRAS*, 348, 187
- Yadav R. K. S., Sagar R. 2001, *MNRAS*, 328, 370